




Experimental study of dripping, jetting and drop-off from thin film flows on inclined fibers

Atefeh Pour Karimi^{1,a} , Manuel Rietz¹, Wilko Rohlf², Benoit Scheid³, and Reinhold Kneer¹

¹ Institute of Heat and Mass Transfer, RWTH Aachen University, Augustinerbach 6, 52056 Aachen, Germany

² Department of Thermal and Fluid Engineering, University of Twente, Drienerlolaan 5, 7522 NB Enschede, The Netherlands

³ TIPS, Université libre de Bruxelles, Avenue F.D. Roosevelt 50, 1050 Bruxelles, Belgium

Received 4 October 2022 / Accepted 30 January 2023 / Published online 9 March 2023

© The Author(s) 2023, corrected publication 2023

Abstract Gravity driven film flows on vertical fibers are known to exhibit a variety of flow dynamics including the formation of droplet trains induced by the hydrodynamic (Kapitza) and Plateau–Rayleigh instability mechanisms. Through an experimental study, it is shown how inclination of the fiber from the vertical influences these dynamics. The formation of waves, regime transitions from dripping to jetting regimes, as well as the onset of drop-off in the form of droplet detachment from the fiber are illustrated and described in dependence of the fiber inclination angle and the liquid mass flow rate. Additionally, the influence of fiber diameter and nozzle geometry on regime transitions and the onset of drop-off from the substrate are examined. It is shown that the onset of drop-off is strongly related to the transition from a regime characterized by a regular wave pattern to a regime characterized by an irregular wave pattern. It is also demonstrated that this regime transition depends not only on flow rate and fiber geometry, but also strongly on the inclination angle. Interestingly, a stabilizing effect of increasing the fiber inclination is detected for constant fiber geometry and film flow rate.

1 Introduction

A liquid film flowing on a thin fiber is a textbook example of a fluid-dynamical system whose evolution is determined by the action of instabilities. In addition to the hydrodynamic [1] and Plateau–Rayleigh [2, 3] instabilities acting on a liquid falling film on a vertical fiber, a thin film on an inclined fiber should also be subject to the Rayleigh–Taylor instability, which should break the radial symmetry and imply the possibility of fluid detachment from the substrate [4]. The formation of waves, their interaction and finally the detachment of droplets from the fiber under the influence of gravity are the result of the occurring instability mechanisms and their interaction. Apart from the theoretical interest, one particular application of liquid films on inclined fibers is the use of fills or wet decks in cooling towers to create a large surface area and thus increase the energy exchange between the cooling liquid and the ambient air flow. A typical design for these surface regions are fills

with a large number of slanted fibers. Further, fog or dew nets used to harvest water in arid regions are often composed of an arrangement of fibers. Water accumulates on those fibers and forms large droplets that slide down to be collected. In such applications, it is not only important to provide a large surface area, but also to control the typical residence time of the liquid on the fiber and to prevent or promote drop-off. Thus, a fundamental understanding of film flow on inclined fibers is important for optimizing such applications. Particularly, parameters such as fiber diameter, the angle of fiber inclination within the structure, and the imposed flow rate are all expected to be the decisive parameters.

Liquid thin films on vertical fibers and related flow regimes have been extensively studied both numerically and experimentally in the past decades [5–9]. Duprat et al. [10] studied the instabilities of viscous film flows on vertical fibers both theoretically and experimentally and introduced flow regimes based on the flow undergoing instability modes. Linear stability analyses of models introduced by Frenkel [11], Kliakhandler [5] and Craster and Matar [12] were performed and their corresponding dispersion relations were derived. Thereby, the transition from absolute to convective regimes and its association with the regular and irregular wavy regimes were inspected. If the growth time

Communicated by Guest editors: Rodica Borcia, Sebastian Popescu, Ion Dan Borcia.

^a e-mail: pour@wsa.rwth-aachen.de (corresponding author)

of the instability (the growth time of the most amplified wave) is smaller than the characteristic time of the wave needed for the advection through its entire wavelength, regular droplet patterns with a defined intrinsic frequency are formed and the instability is said to be absolute. At higher flow rates, the waves are advected faster than they grow leading to convective instability and patterns more subject to irregularities. It has also been reported that when the film is very thin or very thick relative to the fiber radius, the instability is always convective [10]. Only in an intermediate range of film thickness the Plateau–Rayleigh instability dominates the flow and the instability is absolute. Adding to this, it has been shown that the onset of regular and irregular wavy regimes, observed experimentally, coincides precisely with the onset of absolute and convective regimes respectively [13, 14]. Recently, the effect of nozzle geometry on the characteristics of liquid film flows down vertical fibers in the Plateau–Rayleigh regime has been investigated, revealing that the nozzle geometry has a direct impact on the size and frequency of the liquid beads along the fiber [15, 16].

To the best of our knowledge, all the existing studies on film flow on thin fibers are restricted to vertically aligned fibers. There seems to be no study considering inclined fibers with small radius (large curvature) in the Plateau–Rayleigh regime. Existing studies of film flows subject to the Rayleigh–Taylor instability only include film flows under inclined planes [4, 17–22] or inclined or rotating cylinders with diameters equal or larger than 20 mm [23–25]. In this work, we provide experimental data of film flows along inclined thin fibers with a radius $0.05 < R < 0.225$ mm. In such a case, the flow is subject to the hydrodynamic (or Kapitza) instability, to the Plateau–Rayleigh instability due to the strong curvature of the fiber, and to the Rayleigh–Taylor instability due to fiber inclination.

The remainder of this article is structured as follows. In Sect. 2, the experimental setup and procedure are presented. Section 3 introduces the observed flow regimes and provides quantitative results on regime transitions and drop-off mass flow rates depending on the control parameters, i.e. the mass flow rate and fiber inclination. This is followed by a parametric study of the influence of the nozzle and fiber geometry on regime transitions. Finally, the concluding remarks are discussed in Sect. 4.

2 Experimental setup

A schematic illustration of the experimental setup is shown in Fig. 1. A silicone oil v50 (density $\rho = 948$ kg/m³, kinematic viscosity $\nu = 50$ mm²/s, surface tension $\gamma = 0.021$ N/m) flows from the liquid reservoir through a casting nozzle with an inner diameter of $D_{N,i} = 1.5, 1.75, 2.0$ mm and an outer diameter of $D_{N,o} = 2.1, 2.7, 3.3$ mm onto a nylon fiber with diameter $D_f = 0.1, 0.26, 0.45$ mm. The fiber is attached to the container ceiling using a magnet with free movement

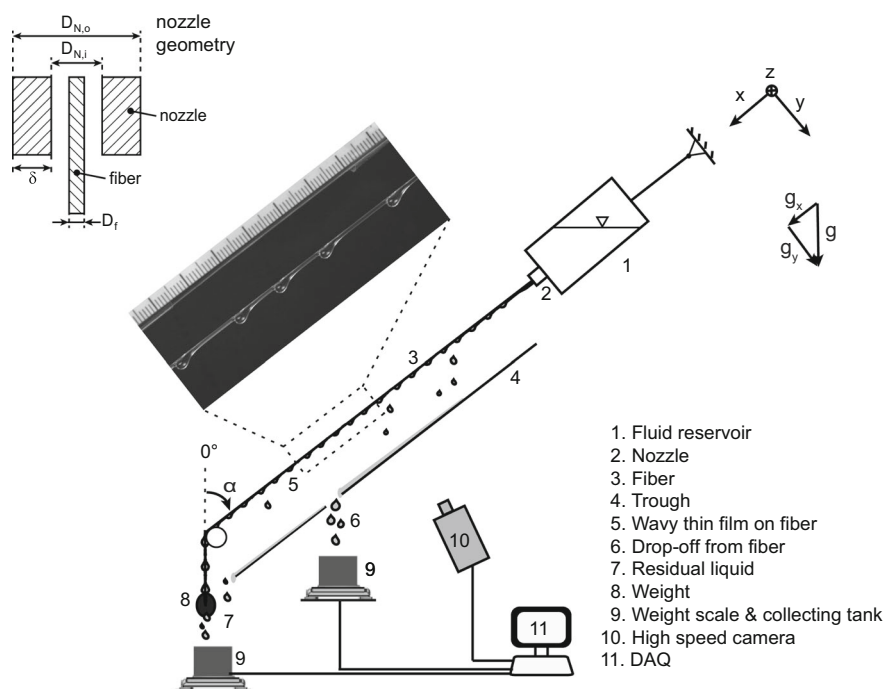
in the Y – Z coordinates and is tensioned by a weight attached to its end. Free movement in the Y – Z coordinates allows the alignment of the fiber in the center of the nozzle and thus guarantees an axisymmetric flow at the nozzle outlet. The whole setup is adjustable for different inclinations from 0° (vertical) to 90° with a step size of 10°. The mass flow rate is adjusted by changing the hydrostatic pressure at the nozzle outlet through variation of the height of the liquid column in the fluid reservoir. The total mass flow rate is measured as the sum of the drop-off and the residual mass flow rate. To measure the current drop-off mass flow, a trough is located under the inclined fiber. The detached droplets drip into the trough and flow into a collecting container located at 80 cm from the nozzle. The collected droplet mass is measured by a weight scale with precision of 0.001 g. A weight scale with a precision of 1 g is used to monitor the residual mass flow rate by measuring the mass of liquid collected in a bucket located under the end of the fiber and trough. The duration of each measurement has been chosen so that it is ensured that the variation of the liquid height in the fluid container is < 1%. Therefore, it can be assumed that the hydrostatic pressure at the nozzle outlet and thus the total mass flow rate are constant. The measurement times are between 20 s up to 4 min, depending on the mass flow rate.

3 Results

3.1 Flow regimes

Figure 2 presents a general overview of the experimentally observed flow patterns on inclined fibers for increasing mass flow rate. Generally, two main regimes are observed for all investigated inclinations, a dripping regime for low mass flow rates and a jetting regime for high mass flow rates. At low flow rates, a dropwise emission, similar to the case of a pendent droplet, is observed at the nozzle. In a repeating process, reminiscent to the quasi-static regime encountered in microfluidic droplet generation [26], fluid accumulates at the nozzle outlet forming a suspended drop. When large enough, the drop detaches from the nozzle and slides down along the fiber in form of a train of isolated waves. This can be referred to the case of the isolated single droplet regime described in previous studies regarding vertical fibers [5, 15], and named the *dripping regime* hereafter.

At high flow rates, a continuous annular jet is formed along the fiber right after the nozzle. After a certain length l_h , this jet destabilizes due to Kapitza instability, Plateau–Rayleigh and Rayleigh–Taylor mechanisms, causing the flow to destabilize into waves. The length l_h through which the perturbations are not visually detectable is called ‘healing length’. In previous studies it has been defined as the length over which the perturbations do not exceed 4% of the uniform film thickness [10]. This regime is referred to the *jetting regime* hereafter, in echo to the dripping to jetting

Fig. 1 Schematic of the experimental setup

transition in microfluidic droplet generation [26], even though waves are produced along the fiber, instead of droplets.

Both the dripping and jetting regimes can further be divided into sub-regimes characterized by regular and irregular wave patterns (see Fig. 2). In the regular wave regime, the waves appear regularly spaced, their amplitude and speed remaining constant over the length of the experimental setup. In the irregular wave regime, the waves no longer are formed periodically at a constant frequency. The size of the waves, their spacing, and frequency vary along the fiber. Variations in size and frequency and therefore wave speed lead to coalescence events, which are not observed in the regular wave sub-regime.

The irregular wave pattern is observed at the lowest flow rates in the dripping regime, while in the jetting regime it is observed at the highest flow rates. In the irregular wave regime, two waves can interact and merge into a wave of larger amplitude. After coalescence, if the wave becomes large enough, it detaches from the fiber under the influence of gravity. For clarity and to avoid ambiguity with the dripping regime from the nozzle, the wave detachment from the fiber substrate is referred hereafter to ‘drop-off’. Actually in the performed experiments, drop-off was only observed in the jetting regime with irregular wave patterns. In the dripping regime and regular wave regimes, drop-off has not been observed along the entire length of the setup for all applied nozzles and fibers. Notice that the occurrence of regular and irregular wave patterns also depends on the length of the domain being analyzed.

All of the observed regimes are in alignment with the regimes detected for the vertical case. In the study

of Duprat et al. [10] it has been shown through stability analysis that regular and irregular wave regimes are associated to an absolute and convective instability, respectively. A transition from convective to absolute and again to convective instability is detected for an increasing flow rate. Based on our observations for the case of an inclined fiber a similar mechanism might be at work. However, a theoretical analysis of the instability modes for a thin film on inclined fibers is out of the scope of the present experimental study.

3.2 Drop-off analysis

Based on our observations, drop-off on inclined fibers occurs due to two main mechanisms (see Fig. 3). The first one is the drop-off as a result of wave interaction of irregular wave patterns at sufficiently large mass flow rates. For low mass flow rates or small inclinations only saturated waves are formed. Even after wave coalescence the waves remain stable and attached to the fiber (see Fig. 3, case 1). However, for increased mass flow rate or inclination, the irregular wave patterns and concomitant wave interactions lead to the formation of large waves undergoing unsaturated growth (see Fig. 3, case 2). The second mechanism is drop-off without wave interaction. In this case, waves undergoing unsaturated growth are formed at the end of the healing length, detaching immediately or after a short march down the fiber without any interaction with other waves (see Fig. 3, case 3). This case is observed at larger inclinations and higher mass flow rates. During the performed experiments for each fiber, a critical angle has been determined at which almost all the liquid immediately detaches, regardless of the selected total mass flow rate (see Fig. 3, case 4). This regime is referred to as

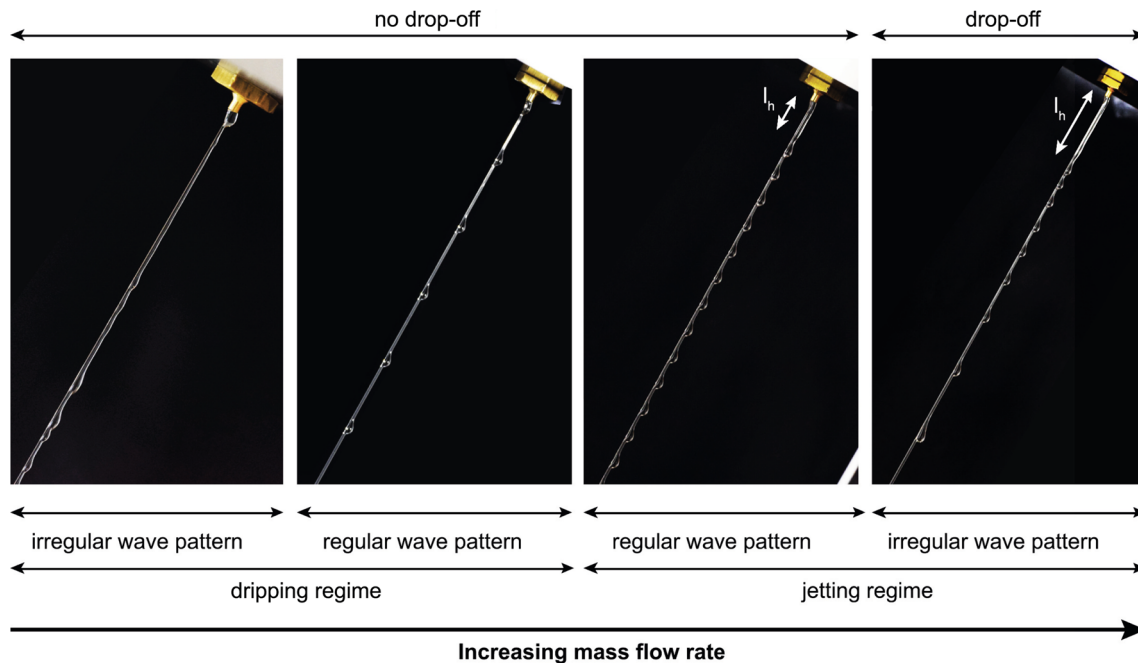


Fig. 2 Observed flow regimes for increasing mass flow rate at 30° inclination; l_h depicts the healing length

‘immediate drop-off’. Figure 3, case 4 shows immediate drop-off without prewetting and a slightly delayed drop-off induced by a forced prewetting of the fiber (compare a and b).

Figure 4 on the first row shows the spatio-temporal plots of the film flow along inclined fibers for the three indicated measurement points 1 to 3 on Fig. 3. It can be seen that for an inclination of 20° (case 1), even after wave coalescence (see blue box), waves are traveling with a constant wave speed of about 0.4 m/s and no drop-off is observed. However, at an inclination of 30° (case 2), the film thickness of the coalesced waves reaches values large enough to induce potential drop-off (as indicated with the green color). This can be seen well at time $t = 0.18$ s and location $x = 8$ cm. It can also be seen that, later downstream, the collision of the residual wave with the next wave also leads to a critical film thickness in green color that characterizes the drop-off event. At 40° inclination (case 3), most of the waves drop off the fiber quickly after the end of the healing length. The power spectrum at a location near the healing length shows for 20° a mean dominant frequency of about 17 Hz (or equivalently a wavelength of 24 mm), without significant harmonic. The dominant frequencies increases with increasing inclination, i.e. 18 Hz for 30° and 21 Hz for 40°. Higher amplitude harmonics for these cases also indicate steeper wave fronts, as expected for larger inclination and flow rate. The last row of graphs in Fig. 4 shows the average film thickness over the entire 1.7 s period at each position on the fiber, starting from the nozzle outlet and continuing 13 cm downstream. Three profile regions can be distinguished: first, a meniscus of large film thickness formed at the nozzle; second, a healing length of constant thickness; third, a region of periodic waves separated by a

thin substrate film thickness. The transitions between the film profile regions are represented roughly by gray dashed lines in the plots. Drop-off occurs mainly in the periodic waves region after some distance equivalent to the healing length. Worth mentioning, in the immediate drop-off regime, drop-off occurs in the meniscus region (not shown).

Figure 5 shows quantitative results of a series of experiments for two different fiber diameters, illustrating the drop-off mass flow rate as a function of total mass flow rate under different inclinations. The highest possible total mass flow rate in each experiment is restricted by the reservoir size. For this reason, larger mass flow rates could be measured for the smallest fiber diameter (Fig. 5b) as the gap between fiber and nozzle at the outlet is the largest. For an inclination of 20°, no drop-off was observed for the fiber with diameter $D_f = 0.45$ mm up to a total mass flow rate of about $\dot{m}_{\text{total}} = 0.30$ g/s. For increasing inclinations drop-off takes place starting from a certain total mass flow rate and its amount increases for an increasing flow rate. Depending on the dominant drop-off mechanism, the increase in drop-off mass flow rate can occur either moderately over a wider range of total mass flow rate or abruptly starting at a certain imposed mass flow rate. This difference in the increase in drop-off mass flow rate is related to whether drop-off occurs primarily by wave interaction (see Fig. 3, case 2) or without wave interaction (see Fig. 3, case 3). Notice, that there exists an intermediate range of mass flow rates in which drop-off can be suppressed by increasing the inclination, roughly for $\dot{m}_{\text{total}} = 0.1$ – 0.2 g/s. As the inclination increases, the onset of drop-off for each inclination is shifted toward higher total flow rates. This is indicated

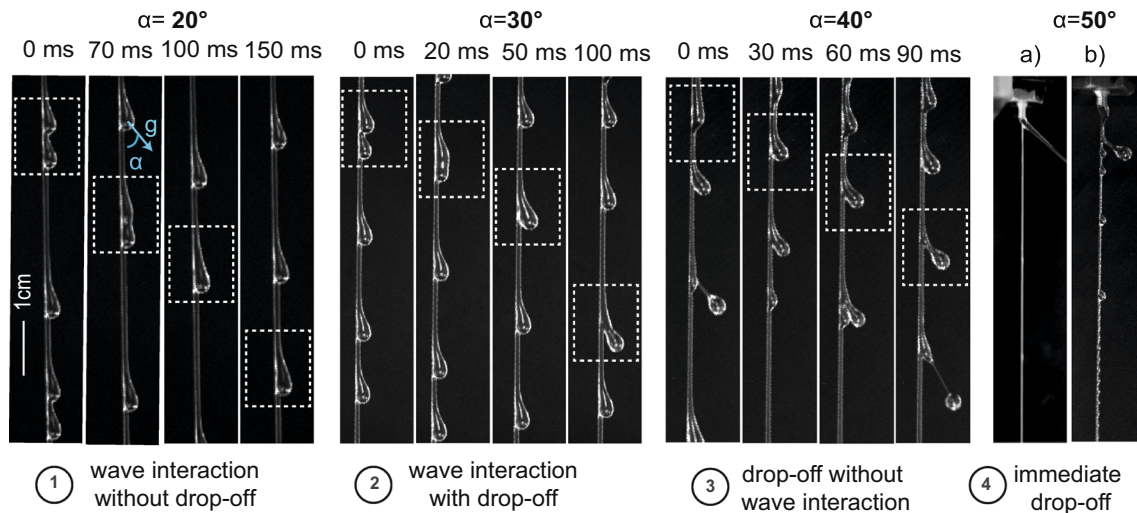


Fig. 3 An overview of observed wave interaction and drop-off mechanisms on fiber $D_f = 0.26$ mm illustrated for inclinations from the vertical ranging from 20° to 50° . For 50° , images a and b are respectively without and with forced prewetting of the fiber. Measurement points and their corresponding mass flow rates can be identified in Fig. 5b

by vertical lines in Fig. 5. The results for 60° inclination in Fig. 5a and 50° inclination in Fig. 5b indicate the critical angle at which the liquid does not adhere to the substrate easily and demands an extra prewetting of the fiber. In this case almost all the liquid drops off immediately regardless of the total flow rate (see Fig. 3, case 4a). A comparison between Fig. 5a, b shows similar trends for increasing mass flow rate, even though it is observed that immediate drop-off takes place at lower inclination for a decreased fiber diameter.

In general, with the exception of the critical inclination for immediate drop-off at the nozzle, we have not observed drop-off at low to moderate mass flow rates in the regular wave regime throughout all of our experiments. Drop-off occurs at higher flow rates in the jetting regime after the flow is transitioned to the irregular wave pattern, where coalescence events lead to growth of the waves and subsequently their detachment from the substrate. Therefore, it seems reasonable to use the transition from regular to irregular wave pattern in the jetting regime as an approximation for the onset of drop-off.

The blue stars and the dashed line in Fig. 6 show the critical mass flow rate at which the transition from a regular wave pattern to an irregular wave pattern occurs for a fiber of $D_f = 0.45$ mm at different inclinations. The color bar illustrates the ratio of drop-off mass flow rate to total mass flow rate, the black color indicating no drop-off and the purple color immediate drop-off at critical inclination. The results illustrate that at larger inclinations the transition from a regular to an irregular wave regime occurs at a higher flow rate, while at the vertical or small inclinations the transition to irregularity occurs at lower flow rates. This is a rather counter intuitive fact indicating that the flow on fibers with larger inclinations remains stable over a wider range of flow rates. Drop-off occurs only after the transition to the irregular wave regime. At the same

time, it is important to notice that for the particular case illustrated in Fig. 6 there exists a threshold angle below which no drop-off was observed, i.e. for $\alpha < 20^\circ$. While certainly no drop-off is expected for the vertical case, it remains unclear whether drop-off might occur for low angles after sufficient fiber length. Nevertheless, the transition from regular to irregular wave pattern in the jetting regime is found to constitute a lower bound for the onset of drop-off up to an angle where less adhesion of fluid to the fiber persists and immediate drop-off occurs.

Duprat et al. [10] have shown for the case of a vertical fiber that the transition to the irregular regime and thus to the drop-off regime in the case of an inclined fiber may correlate with the transition from absolute to convective instability. This transition depends both on the growth rate of the occurring fluid dynamical instabilities as well as on the advection velocity of the perturbations. Both of the mentioned properties are nonlinear functions of flow rate and inclination. The precise description of the phenomena requires a detailed theoretical analysis, which exceeds the scope of this purely experimental study.

3.3 Effect of fiber diameter and nozzle geometry on regime transitions

The direct relationship between the flow regime transition from regular to irregular wave patterns and the onset of drop-off encouraged the investigation of how this regime transition is affected by the geometrical configurations of our setup, namely the sizes of the fiber and of the nozzle.

Figure 7 shows a regime transition map for the same fiber and a variety of nozzle geometries. The study of Sadeghpour [15] showed that varying the nozzle inner diameter has no specific effect on the flow properties

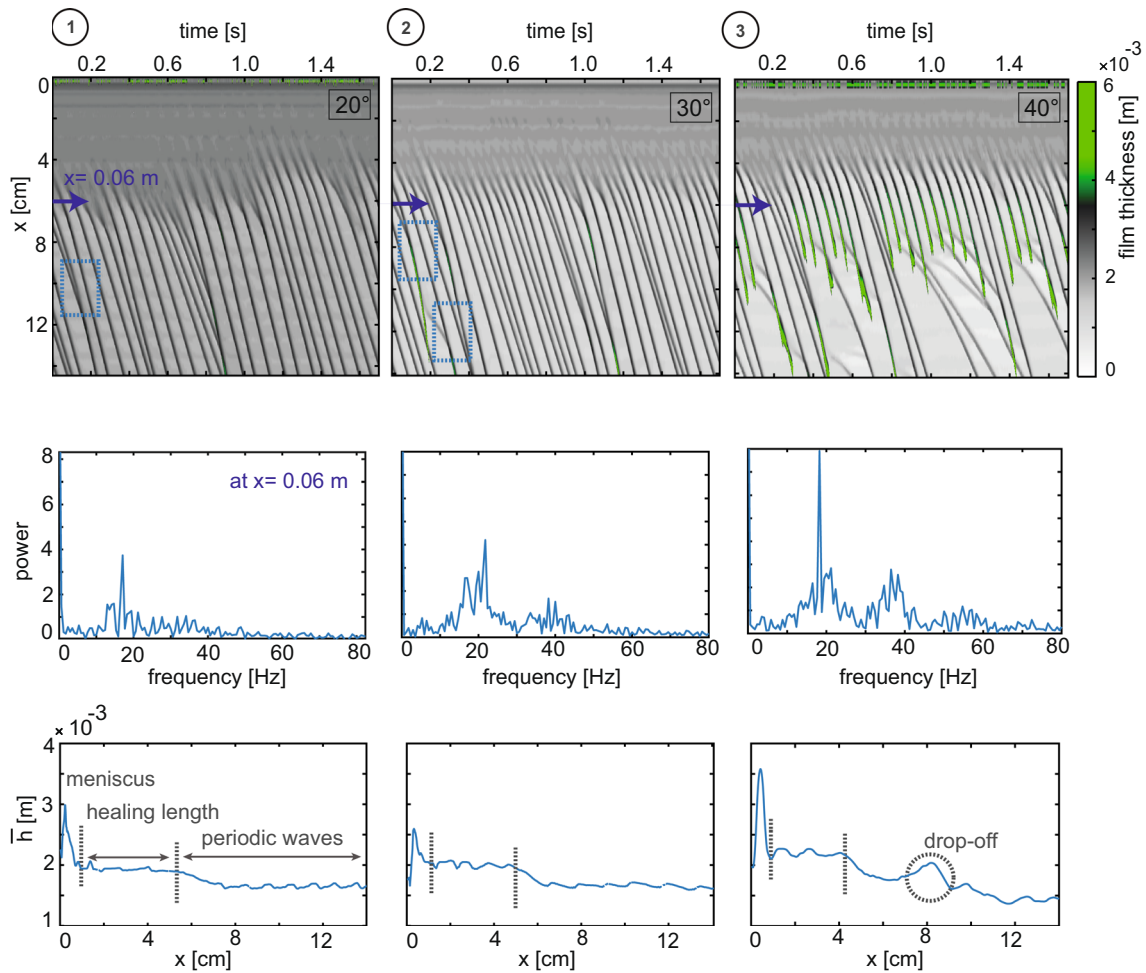


Fig. 4 Spatio-temporal diagrams of film thickness along the fiber for the first three cases as labeled in Figs. 3 and 5b. Blue boxes show coalescence events. The second row shows the corresponding power spectra taken at a fixed location as indicated by the blue arrows. The third row show the temporal integration over the time interval of 1.7 s of the film thickness along the fiber. Gray dash lines shows the transitions between the three profile regions along the coated fiber. The temporal and spatial resolutions of the analyzed images are 1 ms and 0.17 mm, respectively

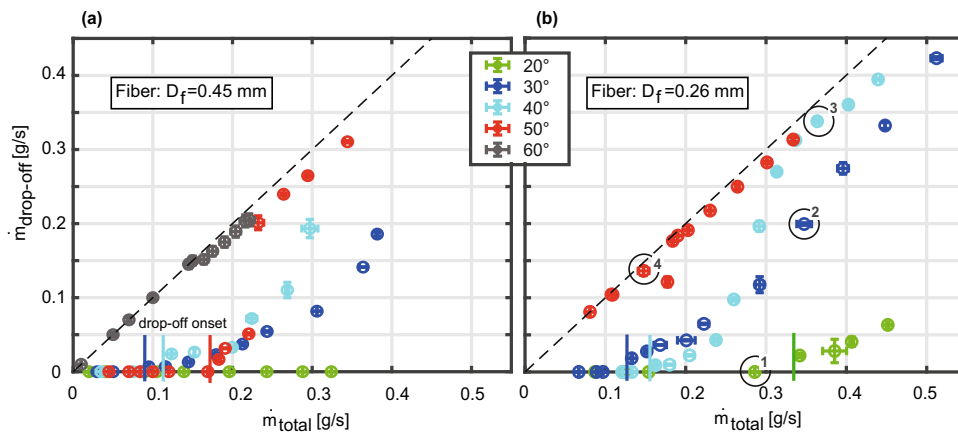


Fig. 5 Drop-off mass flow rates are shown as a function of the total mass flow rate and the inclination angle for fiber diameters **a** $D_f = 0.45$ mm and **b** $D_f = 0.26$ mm. The inner and outer diameters of the nozzle applied for both fibers are $D_{N,i} = 1.5$ mm, $D_{N,o} = 2.1$ mm. The onset of drop-off for each inclination is shown in both figures through vertical lines with the same color reference according to the legend. Images corresponding to measurement points labeled 1 to 4 are shown in Fig. 3

Fig. 6 Drop-off mass flow rate in dependence of total mass flow rate \dot{m}_{total} and inclination angle α for $D_f = 0.45$ mm. Blue stars and dashed line indicate the sub-regime transition from regular to irregular wave pattern within the jetting regime. Purple squares indicate immediate drop-off regime. The color chart shows the normalized droplet mass flow to the total mass flow rate. Black dots indicate the measuring points without drop-off

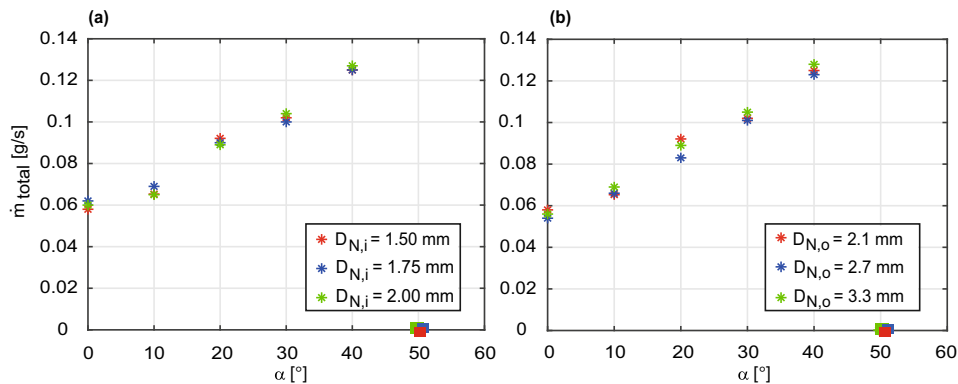
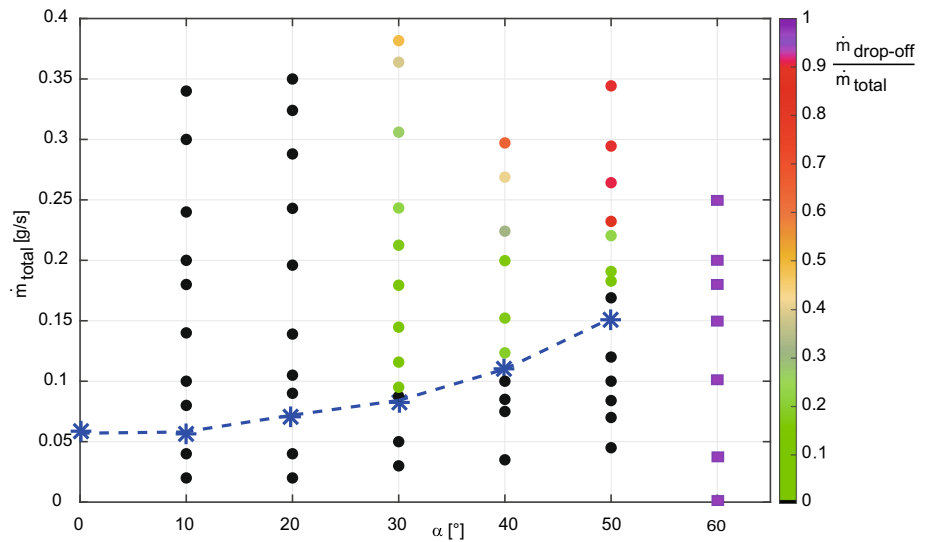


Fig. 7 Sub-regime transition from regular to irregular wave pattern within the jetting regime for different nozzle geometries with a constant fiber diameter of $D_f = 0.26$ mm. Squares indicate immediate drop-off regime for each corresponding nozzle. **a** Nozzles with a constant wall thickness of $\delta = 0.3$ mm and increasing nozzle inner diameter. **b** Nozzles with a constant inner diameter of $D_{N,i} = 1.5$ mm and increasing wall thickness $\delta = 0.3, 0.6, 0.9$ mm

on the fiber and only the nozzle outer diameter is the influencing nozzle parameter. Also, studying the transition from dripping regime to jetting on stainless steel tubes, Clanet and Lasheras [27] considered the outer diameter of the nozzle as the characteristic parameter since the fluid at the nozzle exit always wets the tube frontal area up to the outer diameter. For this reason, a variety of nozzle geometries are examined, which always included a change in the nozzle outer diameter. Figure 7a compares the results for the cases where the nozzle inner diameter increases while the wall thickness remains constant. Figure 7b displays the results for the case where the nozzle inner diameter is kept constant and the wall thickness increases. As it can be seen from the graphs, the variation in the results is trivial for all nozzle geometries, such that the outcome suggests that nozzle geometry is not a determining variable for transition from regular to irregular wave pattern in flows under inclined fibers. One possible reason for that might be that the examined transition occurs in the jetting regime. Therefore, the influence of the nozzle geometry

can be suppressed through the extension of the existing healing length.

Figure 8 shows the regime transition map for three different fibers ($D_f = 0.1, 0.26, 0.45$ mm) and a constant nozzle ($D_{N,i} = 1.75$ mm, $D_{N,o} = 2.1$ mm). It is evident that for small inclinations from the vertical, the smaller fibers have the most stable flow, and for larger inclinations, the larger fibers are most likely to resist instability and drop-off at higher mass flow rates. Getting back to the above-mentioned examples of application, when designing and optimizing wet decks in cooling towers or fog/dew collection nets, this regime map can provide an overview for selecting the appropriate geometric parameters including the size of the fiber and its inclination based on the selected flow conditions.

4 Conclusion

This study investigates the flow characteristics and drop-off of a falling liquid film on inclined fibers with a diameter in the range of $D_f =$

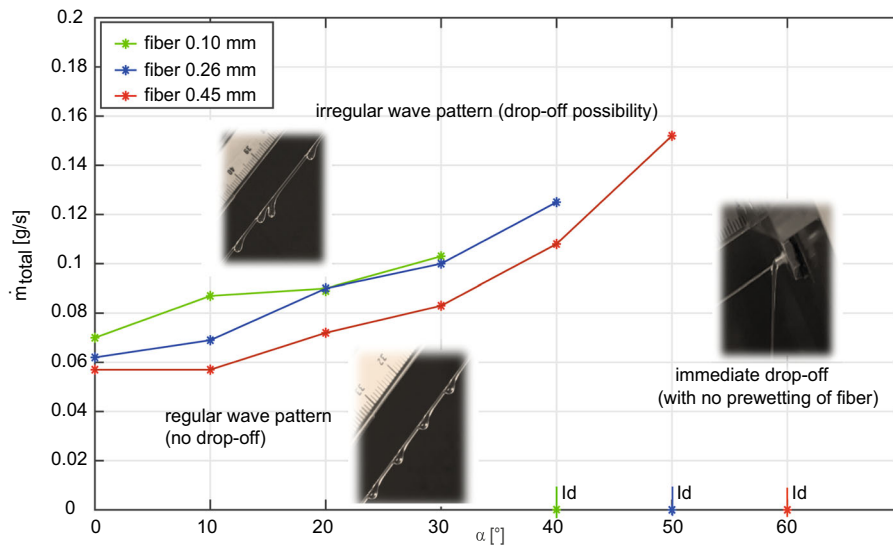


Fig. 8 Sub-regime transition from regular to irregular wave pattern within the jetting regime for three different fiber diameters ($D_f = 0.1, 0.26, 0.45$ mm) and a nozzle with inner and outer diameter of $D_{N,i} = 1.75$ mm, $D_{N,o} = 2.1$ mm. The three plotted lines indicate the transition lines from jetting regular to irregular regime. The colored vertical lines on the x-axis show the critical inclination for each fiber, from which the immediate drop-off regime begins. The images illustrate examples of flows in jetting-regular, jetting-irregular as well as immediate drop-off regimes in their approximate flow rate range

0.1–0.45 mm, where the Plateau–Rayleigh and the Rayleigh–Taylor instabilities are the dominant instability mechanisms in addition to the Kapitza instability. Several physical parameters that impose and influence the drop-off events on inclined fibers such as the total mass flow rate at the nozzle outlet, the fiber inclination from the vertical as well as the fiber diameter and the nozzle geometry are examined and reported. It is shown that, for a constant geometry, the drop-off mass flow rate increases with an increasing mass flow rate at the nozzle outlet. However, this increase does not follow a linear trajectory, but rather proceeds in a more nonlinear manner. Different drop-off mechanisms, strongly influenced by the angle of inclination, can lead to different responses of the drop-off mass flow rate as a function of the total mass flow rate. It is observed that in contrary to the planar case, where an increasing negative inclination leads to an increasing instability and an increasing drop-off mass flow rate [17, 20], for a curved substrate like a fiber, an increasing inclination can have stabilizing effects. A critical inclination is introduced, from which the liquid would even after a forced pre-wetting of the fiber no longer stick to the fiber and would immediately drop off. Immediate drop-off at critical inclination is independent of the flow parameters. However, at all inclinations smaller than the critical inclination, all drop-off mechanisms are observed only in the jetting regime with irregular wave patterns. The transition from regular wave pattern in the jetting regime to irregular wave pattern has been shown to occur at higher total mass flow rates for an increasing fiber inclination. This implies that at higher inclination the flow remains stable and is resistant to drop-off for a larger range of total mass flow

rate. Finally, the influence of the nozzle geometry and the fiber diameter on the existing flow regimes and thus on drop-off is presented. It is shown that the nozzle geometry is not a determining parameter in the flow regime transition and thus the drop-off on the fiber. However, the fiber diameter, along with the total flow rate and the fiber inclination, proves to be a characteristic parameter that strongly influences the drop-off phenomena on inclined fibers.

Funding Open Access funding enabled and organized by Projekt DEAL. Funding for A.P.K. was provided by DFG (Deutsche Forschungsgemeinschaft) under reference number 418676633. B.S. thanks the F.R.S.-FNRS for funding.

Data availability The datasets generated during and/or analysed during the current study are available from the corresponding author on reasonable request.

Declarations

Conflict of interest The authors have no competing interests to declare that are relevant to the content of this article.

Open Access This article is licensed under a Creative Commons Attribution 4.0 International License, which permits use, sharing, adaptation, distribution and reproduction in any medium or format, as long as you give appropriate credit to the original author(s) and the source, provide a link to the Creative Commons licence, and indicate if changes were made. The images or other third party material in this article are included in the article's Creative Commons licence, unless indicated otherwise in a credit line to the material. If material is not included in the article's Creative Commons licence and

your intended use is not permitted by statutory regulation or exceeds the permitted use, you will need to obtain permission directly from the copyright holder. To view a copy of this licence, visit <http://creativecommons.org/licenses/by/4.0/>.

References

- P. L. Kapitza, Wave flow of thin layer of viscous fluid. *J. Exp. Theor. Phys.* **18** (1948) (in Russian)
- J. Eggers, Nonlinear dynamics and breakup of free-surface flows. *Rev. Mod. Phys.* **69**(3), 865–930 (1997). <https://doi.org/10.1103/RevModPhys.69.865>
- D.T. Papageorgiou, On the breakup of viscous liquid threads. *Phys. Fluids* **7**(7), 1529–1544 (1995). <https://doi.org/10.1063/1.868540>
- A. Indeikina, I. Veretennikov, H.-C. Chang, Drop fall-off from pendent rivulets. *J. Fluid Mech.* **338**, 173–201 (1997)
- I.L. Kliakhandler, S.H. Davis, S.G. Bankoff, Viscous beads on vertical fibre. *J. Fluid Mech.* **429**, 381–390 (2001). <https://doi.org/10.1017/S0022112000003268>
- S.V. Alekseenko, V.E. Nakoryakov, B.G. Pokusaev, Wave formation on vertical falling liquid films. *Int. J. Multiph. Flow* **11**(5), 607–627 (1985). [https://doi.org/10.1016/0301-9322\(85\)90082-5](https://doi.org/10.1016/0301-9322(85)90082-5)
- S. Kalliadasis, H.-C. Chang, Drop formation during coating of vertical fibres. *J. Fluid Mech.* **261**, 135–168 (1994). <https://doi.org/10.1017/S0022112094000297>
- C. Ruyer-Quil, S. Kalliadasis, Wavy regimes of film flow down a fiber. *Phys. Rev. E Stat. Nonlinear Soft Matter Phys.* **85**(4Pt 2), 046302 (2012). <https://doi.org/10.1103/PhysRevE.85.046302>
- D. Quéré, Thin films flowing on vertical fibers. *Europhys. Lett.* **13**(8), 721–726 (1990). <https://doi.org/10.1209/0295-5075/13/8/009>
- C. Duprat, C. Ruyer-Quil, S. Kalliadasis, F. Giorgiutti-Dauphiné, Absolute and convective instabilities of a viscous film flowing down a vertical fiber. *Phys. Rev. Lett.* **98**(24), 244502 (2007). <https://doi.org/10.1103/PhysRevLett.98.244502>
- A.L. Frenkel, Nonlinear theory of strongly undulating thin films flowing down vertical cylinders. *Europhys. Lett.* **18**(7), 583–588 (1992). <https://doi.org/10.1209/0295-5075/18/7/003>
- R.V. Craster, O.K. Matar, On viscous beads flowing down a vertical fibre. *J. Fluid Mech.* **553**(1), 85 (2006). <https://doi.org/10.1017/S0022112006008706>
- C. Duprat, C. Ruyer-Quil, F. Giorgiutti-Dauphiné, Spatial evolution of a film flowing down a fiber. *Phys. Fluids* **21**(4), 042109 (2009). <https://doi.org/10.1063/1.3119811>
- C. Duprat, C. Ruyer-Quil, F. Giorgiutti-Dauphiné, Experimental study of the instability of a film flowing down a vertical fiber. *Eur. Phys. J. Spec. Top.* **166**(1), 63–66 (2009). <https://doi.org/10.1140/epjst/e2009-00879-9>
- A. Sadeghpour, Z. Zeng, Y.S. Ju, Effects of nozzle geometry on the fluid dynamics of thin liquid films flowing down vertical strings in the Rayleigh-plateau regime. *Langmuir ACS J. Surf. Colloids* **33**(25), 6292–6299 (2017). <https://doi.org/10.1021/acs.langmuir.7b01277>
- H. Ji, A. Sadeghpour, Y.S. Ju, A.L. Bertozzi, Modelling film flows down a fibre influenced by nozzle geometry. *J. Fluid Mech.* (2020). <https://doi.org/10.1017/jfm.2020.605>
- P.-T. Brun, A. Damiano, P. Rieu, G. Balestra, F. Gallaire, Rayleigh–Taylor instability under an inclined plane. *Phys. Fluids* **27**(8), 084107 (2015). <https://doi.org/10.1063/1.4927857>
- B. Scheid, N. Kofman, W. Rohlf, Critical inclination for absolute/convective instability transition in inverted falling films. *Phys. Fluids* **28**(4), 044107 (2016). <https://doi.org/10.1063/1.4946827>
- W. Rohlf, P. Pischke, B. Scheid, Hydrodynamic waves in films flowing under an inclined plane. *Phys. Rev. Fluids* **2**, 4 (2017). <https://doi.org/10.1103/PhysRevFluids.2.044003>
- F.F. Abdelall, S.I. Abdel-Khalik, D.L. Sadowski, S. Shin, M. Yoda, On the Rayleigh–Taylor instability for confined liquid films with injection through the bounding surfaces. *Int. J. Heat Mass Transf.* **49**(7–8), 1529–1546 (2006). <https://doi.org/10.1016/j.ijheatmasstransfer.2005.07.055>
- N. Kofman, W. Rohlf, F. Gallaire, B. Scheid, C. Ruyer-Quil, Prediction of two-dimensional dripping onset of a liquid film under an inclined plane. *Int. J. Multiph. Flow* **104**, 286–293 (2018). <https://doi.org/10.1016/j.ijmultiphaseflow.2018.02.007>
- G. Zhou, A. Prosperetti, Dripping instability of a two-dimensional liquid film under an inclined plate. *J. Fluid Mech.* (2022). <https://doi.org/10.1017/jfm.2021.1032>
- S. Aktershev, S. Alekseenko, A. Bobylev, Waves in a rivulet falling down an inclined cylinder. *AIChE J.* **67**, 1 (2021). <https://doi.org/10.1002/aic.17002>
- S.V. Alekseenko, A.V. Bobylev, D.M. Markovich, Rivulet flow on the outer surface of an inclined cylinder. *J. Eng. Thermophys.* **17**(4), 259–272 (2008). <https://doi.org/10.1134/S1810232808040012>
- M. Rietz, B. Scheid, F. Gallaire, N. Kofman, R. Kneer, W. Rohlf, Dynamics of falling films on the outside of a vertical rotating cylinder: waves, rivulets and dripping transitions. *J. Fluid Mech.* **832**, 189–211 (2017). <https://doi.org/10.1017/jfm.2017.657>
- A. Dewandre, J. Rivero-Rodriguez, Y. Vitry, B. Sobac, B. Scheid, Microfluidic droplet generation based on non-embedded co-flow-focusing using 3d printed nozzle. *Sci. Rep.* **10**, 21616 (2020). <https://doi.org/10.1038/s41598-020-77836-y>
- C. Clanet, J.C. Lasheras, Transition from dripping to jetting. *J. Fluid Mech.* **383**, 307–326 (1999). <https://doi.org/10.1017/S0022112098004066>